S. Hager, M. Meinardus, T. Hofmann and K. Glas

$CaCO_3$ deposits in reverse osmosis: Part II – Simulation model for hydrochemical predictions of reverse osmosis retentates and scaling propensity

Reverse osmosis (RO) technology is used in a wide variety of water treatment processes. In the brewing industry, mainly for the production of brewing and process water. The design and resulting efficiency of RO plants depends on hydro chemical predictions of the retentate flow. In order to avoid deposits in the membrane system, saturation limits of sparingly soluble salts are of decisive importance when selecting the maximum achievable fresh water yield. For the frequently present calcium carbonate ($CaCO_3$), predictive indices of calcite saturation such as the Langelier saturation index (LSI) are widely used. However, due to simplifications of the water chemistry, the prediction quality must be critically questioned. In this context, we present a new simulation model for predicting RO retentate water chemistry. The calculations are performed in the freely available hydrochemical simulation software PHREEQC. Using a validation data set from German standard methods (DIN) for the determination of calcite saturations, a good agreement could be achieved with our calculation basis in PHREEQC software. The simplified description of LSI values from the ASTM International Standard and software from a membrane manufacturer provided greatly increased calcite saturations in comparison. In addition to the consideration of calcite saturation, we were able to extend our prediction of RO retentates to the saturations of further $CaCO_3$ polymorphs as the monohydrate (MCC) and in the amorphous form (ACC). This allows us to reveal, for example, a metastable range of $CaCO_3$ supersaturation as a function of the raw water recovery rate. Previously difficult-to-explain scaling behaviour of RO systems at high calcite supersaturation could be explained using this approach. The prediction of the retentate pH value and thus the membrane rejection of carbon in the membrane system showed good agreement with full scale data when simulating constant CO_2 concentration independent of fresh water yield. Today, the hydrochemical design of reverse osmosis systems is usually based on unpublished calculation methods of membrane manufacturers, chemical suppliers and the ASTM guidelines. With our simulation approach, these predictions can be critically evaluated and comprehensive RO design calculations can be modularly coupled with our interface open simulation model in PHREEQC.

Descriptors: scaling, $CaCO_3$, LSI, fouling, reverse osmosis, pH prediction, Langelier Saturation Index

1 Introduction

In part I [1] of this publication series, the possibilities and reasons for describing calcite saturation in RO systems were presented in detail. In this publication, the findings from Part I are transferred to calculation results from our simulation approach, which has already been partly presented. The main motivation for the present work lies in the balancing act that must be ensured for a resource-saving and cost-effective operation of reverse osmosis plants. On the one hand, the yield and operational safety should meet the highest demands, on the other hand, a reduced use of chemicals is preferable. Thereby, the precipitation and stabilization of sparingly soluble salts in the membrane system is of particular interest. Correct prediction of saturation of the most frequent precipitate $CaCO_3$ is of great importance for this purpose. Today, the Langelier Saturation Index LSI is frequently applied. It is mainly determined according to a calculation method from the ASTM international standards [2–9] as an extension of the original description according to Langelier [10]. In addition, manufacturers or distributors of membranes and chemicals offer their own software to predict the concentrated RO retentate in terms of salt saturation [11]. The chemical changes of the water during the reverse osmosis process are thus represented and ultimately serve the plant design. Further methods for the determination of $CaCO_3$ saturation and therefore probability of the blockage of $CaCO_3$ scaling were reviewed in part I [1]. The basis for an accurate calculation of the hydro chemistry

https://doi.org/10.23763/BrSc22-07hager

Authors

Simon Hager, Thomas Hofmann, Karl Glas, Water Systems Engineering, Chair of Food Chemistry and Molecular Sensory Science, TUM School of Life Sciences, Technische Universität München, Freising, Germany; Martin Meinardus, Grünbeck Wasseraufbereitung GmbH, Höchstädt, Germany; corresponding author: simon.hager@tum.de

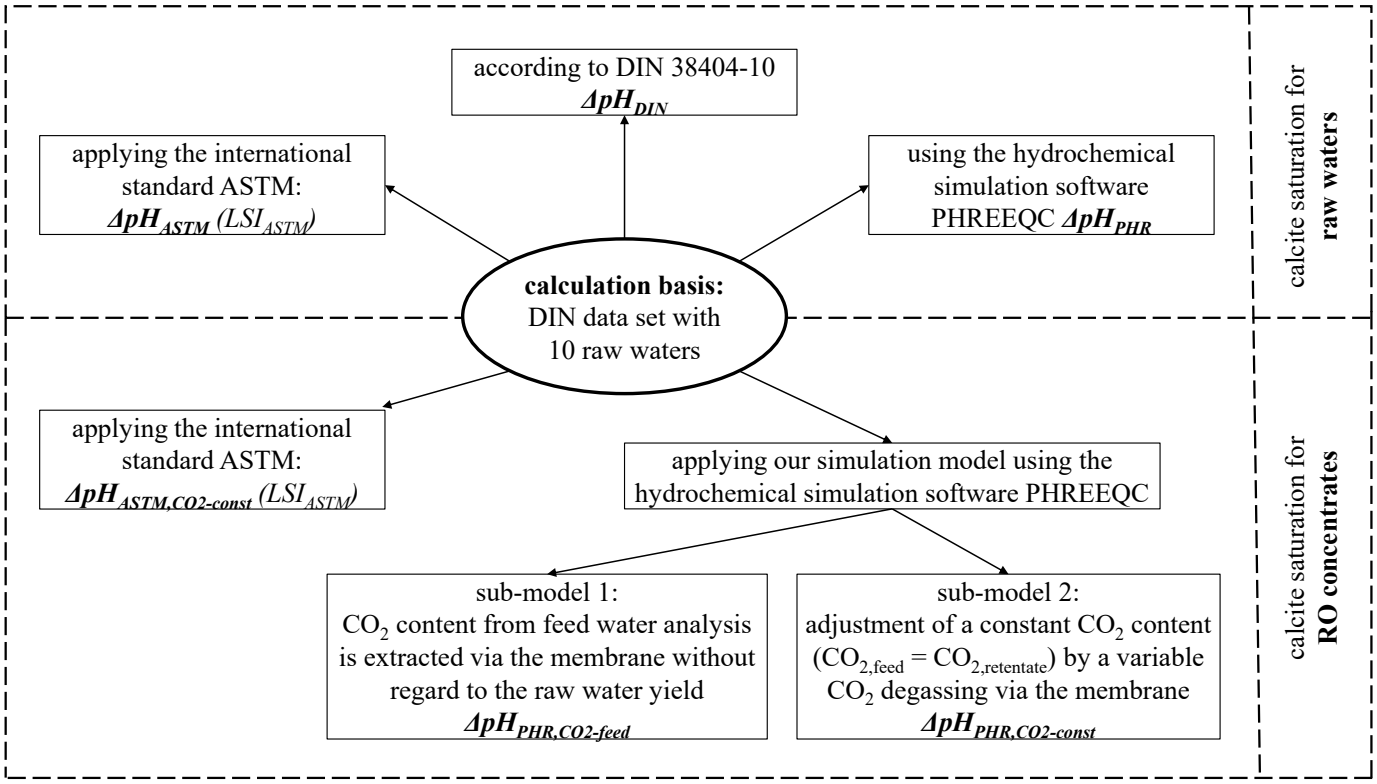

Fig. 1 Utilization of the raw water samples from the DIN data set for comparison and validation of different calculation methods for the determination of calcite saturation and LSI values

and especially carbonate chemistry is the correct prediction of the carbon rejection in the membrane system and therefore the pH value of the retentate stream. This relationship is of particular interest, since $CaCO_3$ saturation is strongly dependent on the pH value and the corresponding CO_3^{-2} concentration. Various methods for pH prediction of RO retentates have already been explored in the literature. Previously, a strong influence on the design and the required chemical input could be demonstrated and that the $CaCO_3$ saturation and thus the precipitation risk is often overestimated [12, 13]. Our approach is to quantitatively demonstrate these uncertainties associated with the conventional saturation description of the LSI and to provide an easy-to-use alternative with our simulation model. Furthermore, this open interface and freely available model in the simulation software PHRREQC [14] is intended to enable the coupling to further scientific work, e.g. in the field of multiphysics simulations. In order to make the conventional LSI or S&DSI data comparable with our approach, our method was developed in such a way that the $CaCO_3$ saturation is also expressed in pH values [1]. For this purpose, the current standard procedures for describing $CaCO_3$ saturation according to the ASTM International and the Deutsche Industrie Norm (DIN) are first compared with our model in the following. Subsequently, full scale RO data are used to interpret our model in terms of pH prediction and finally the onset of $CaCO_3$ scaling. Like the LSI, our model is also based on the description of $CaCO_3$ saturations. The correct calculation of this parameter is crucial for a correct prediction of $CaCO_3$ precipitation and scaling. However, there are further additional influences that make an accurate prediction of the actual onset of $CaCO_3$ scaling impossible so far. Some of these influences are discussed at the end of this article as well as in the literature [15]. The following publication, part III, therefore addresses the early detection of scaling and presents experimental results using an optical polymer sensor in a reverse osmosis system that could help monitor and understand the complex scaling phenomena.

2 Materials and Methods

This work focuses on predictive calculations for the water chemistry of RO retentates. First the prediction of $CaCO_3$ saturation is considered in a simulative part and then the calculations are transferred to reanalysed data of a full-scale RO system. The basic description of $CaCO_3$ saturation and in particular of calcite saturation is done in this work by means of the ΔpH value, which is determined according to the following Equation 1. It is based on the actual or predicted pH-value of the water to be evaluated and the pH-value in the equilibrium state of $CaCO_3$, pH_S. When applying this approach to calcite as the most stable $CaCO_3$ polymorph, Equation 1 leads to the widely applied LSI [1].

$$\Delta pH_{calcite} = pH_{measured/predicted} - pH_{S,calcite} = LSI \quad \text{(Eq. 1)}$$

2.1 Calculation methods for calcite saturation and structure of comparative analyses

As shown in the figure 1, the basis of the first part of this work are calculations based on 10 raw water samples of a DIN validation data set (Table 1, see page 56) on the prediction of calcite saturation [16]. The results of the DIN are compared with our calculation approach and the international standard ASTM. For the prediction of RO retentates, the DIN does not provide a method or validation data. Therefore, in a second step, our prediction approach is compared only with the ASTM [9] which was developed specifically

Table 1 Validation water samples from the German Industry Standard methods DIN 38404-10 for the computation of calcite saturation and subsequent comparative analyses of the different calculation methods

		Water sample									
Paramter	**Unit**	**1**	**2**	**3**	**4**	**5**	**6**	**7**	**8**	**9**	**10**
Calcium	mmol/L	1.40	0.75	3.50	0.15	1.40	0.78	1.30	1.00	2.65	1.00
Magnesium	mmol/L	0.23	0.10	0.70	0.05	0.25	0.10	0.25	0.25	0.20	0.18
Sodium	mmol/L	0.30	0.40	2.30	0.30	0.40	0.45	1.60	0.20	0.30	0.20
Potassium	mmol/L	0.05	0.10	0.30	0.10	0.07	0.05	0.15	0.06	0.06	0.05
Carbon (DIC)	mmol/L	2.74	1.63	6.72	1.38	2.66	1.58	1.16	2.09	4.67	2.06
Chloride	mmol/L	0.25	0.30	2.70	0.34	0.55	0.28	0.85	0.35	0.75	0.10
Nitrate	mmol/L	0.15	0.03	0.50	0.18	0.20	0.00	0.10	0.05	0.05	0.05
Sulfate	mmol/L	0.38	0.15	1.20	0.05	0.25	0.15	1.40	0.20	0.55	0.25
Phosphate	mmol/L	0.00	0.00	0.00	0.00	0.07	0.07	0.00	0.03	0.00	0.03
Temperature	°C	10.0	15.0	10.0	10.0	10.0	15.0	12.0	10.0	15.0	61.0
pH	–	7.34	7.80	7.00	5.60	7.37	7.86	7.59	7.47	7.30	7.30

for this prediction purpose. Here, different approaches to describe CO_2 degassing (and therefore carbon rejection or passage) are investigated using two different sub-models. As no substantial gas rejection of RO membranes is to be expected [3] the degassing of CO_2 from the feed stream is a reasonable approach with sub-model 1. Sub-model 2 follows the ASTM method by assuming a constant CO_2 concentration in the retentate stream, independent of raw water recovery rate.

The calcite saturations determined according to ASTM are based on the application of the formulas and graphical interpolations as named in the ASTM publications. The calcite saturations calculated according to the DIN method are reported for in the validation data set in the form of the pH and pHS values. Our simulation model and therefore calcite saturations are calculated with the freely available hydrochemical simulation software PHREEQC as described below.

2.2 Detailed description of our calculation model, simulation software PHREEQC and its parameterization

Our model applied in the present study is calculated with the software PHREEQC version 3.6.4. It is provided free of charge by the United States Geological Survey. In the current version 13 different databases are integrated, which serve different purposes. Variations lie in the thermodynamic principles that are used for the calculation. In particular, this concerns the type and number of defined chemical species, the temperature correction of the equilibrium constants and the correction of the reactive concentration fractions by applying different activity coefficient models. For the calculations carried out in this study, the default database preeqc.dat was used. Activity coefficients are calculated using the extended Debye-Hückel Theory. This theory is valid up to an ionic strength 100 mmoL/L [17] and thus encompasses the ionic strengths encountered in this work. The presented model can also be suitable for higher salinity waters and higher recovery rates (ionic strength > 100 mmoL/L) by an appropriate variation of the database. For example, the calculation of the activity coefficients can be performed using the basic principles of *Pitz*er et al. [18]. For this purpose, e.g. the database pitzer.dat can be chosen. However, the chemical species represented in the database should first be harmonized with the constituents of the respective water analysis. Especially for $CaCO_3$ important ion-pair and complexation reactions are missing in the pitzer.dat database. The selection of a suitable database should always be done carefully and the proper selection has recently been described in the literature [19]. In the simulations we performed, important species of the calcium and carbonate chemistry are included in the phreeqc.dat database, as they are also listed in the DIN. In addition to the dissociation reactions of carbonate, sulphates and phosphates as well as dissolved ion-pair bonds and complexation reactions are particularly worth mentioning (e.g.: $CaCO_3^0$, $CaSO4^0$, $MgCO_3^0$, $Ca(OH)^+$, $Mg(OH)^+$, etc.). The temperature dependence of the applied equilibrium constants is determined with empirical data sets, if available. Otherwise, these corrections are calculated using the Van't Hoff equation and reaction enthalpies, all listed in the applied database. These applied physicochemical calculations are largely similar to the approaches in the DIN [20], in which the calculations for the chemistry of calcium carbonate are presented transparently. The calculations with PHREEQC are not limited to $CaCO_3$, and thus, for example, suitable for the calculation of the supersaturation of other potential scalants, e.g. sulphates and phosphates such as the widespread salt precipitation, e.g. $BaSO_4$, $SrSO_4$ or various apatites. An important feature of the PHREEQC software is the possibility of iterative calculation of equilibrium reactions under inclusion of defined CO_2 contents. Thus, a calculation of CO_2 degassing in membrane processes with simultaneous calculation of increasing raw water salinity becomes possible. Due to the carbonate chemistry, variations in the CO_2 concentration lead to a shift in the pH value. Such effects are widely known in reverse osmosis applications [12]. The pH and especially the related CO_3^{-2} concentration is essential for the calculation and prediction of $CaCO_3$ formation. Our model is divided into two sub-models, as shown in figure 1 and outlined in more detail in figure 2. Both approaches are based on rather simple assumptions of a complete and recovery-independent CO_2 removal or a constant CO_2 content from the raw water inlet to the retentate outlet. The quality of the CO_2 simulation can be evaluated by pH measurements on real membrane processes and is represented basically via the reac-

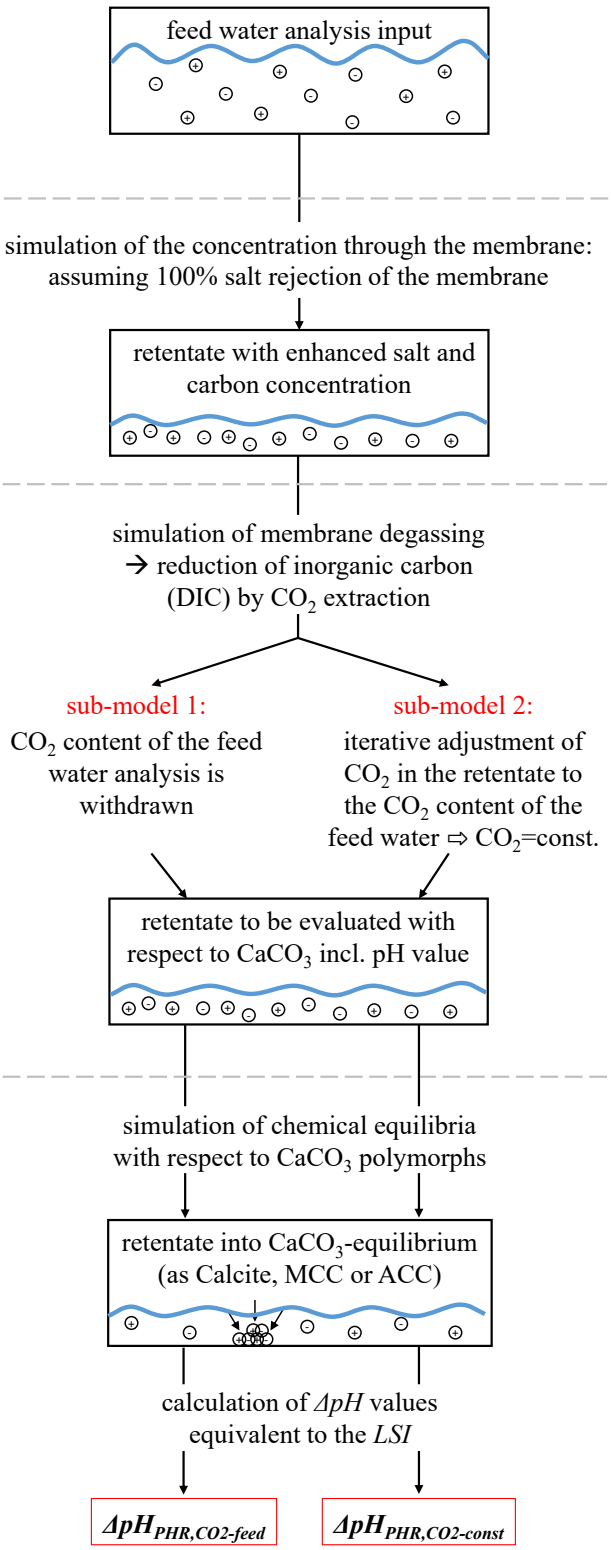


```
SOLUTION 1 feed_water_input
pH 7.31;  temp 12.2;  units mg/L
Ca 120; Mg 19; Na 5.6; K 1.4
Cl 25; N(5) 30 as NO3-; S(6) 27 as SO4-2
alkalinity 372 as HCO3-
END
#Output: e.g. CO2 concentration of feed water

USE SOLUTION 1 pure_water_extraction
REACTION; H2O -1.0; 43.298 moles
SAVE solution 11
END
#Phreeq calculates a solution as 1 kg water
containing 55.51 moles pure H20. For example,
a feed water recovery of 78% results in 43.298
moles H20 to be withdrawn.

#sub-model 1:
USE SOLUTION 11 extraction_of_CO2_feed
REACTION; CO2 -7.239e-04
SAVE solution 111
END
#value derived from feed water CO2 SOLUTION 1 as
CO2[mol/kg]

#sub-model 2:
USE SOLUTION 11 CO2_adjusted_to_feed_water_level
EQUILIBRIUM_PHASES; Fix_CO2 -3.1403
SAVE solution 111
END
#value derived from feed water CO2 SOLUTION 1
log(-CO2[mol/kg]) -> log(-7.239e-04)=-3.1403

#Output:  predicted pH value of the retentate
#Output:  saturation S and SI values for defined
          CaCO3 polymorphs (Calcite, MCC, ACC)

USE solution 111 set_equilibrium_calcite
EQUILIBRIUM_PHASES; Calcite 0.0  ;END

USE solution 111 set_equilibrium_monohydrate
EQUILIBRIUM_PHASES; MCC 0.0      ;END

USE solution 111 set_equilibrium_amorphous
EQUILIBRIUM_PHASES; ACC 0.0      ;END

#Output:  pH values at CaCO3 saturation of
          specific polymorph pHs

#Final calculations: pH(predicted) - pHs = ΔpH
```

Fig. 2 **Main part of our simulation model for predicting the $CaCO_3$ saturation and water chemistry of reverse osmosis retentates. Left: Structure of the simulation model. Right: Related PHREEQC code for the exemplary calculation of the water chemistry to the evaluated full-scale RO data. The two different sub-models, for describing CO_2 permeation through the membrane are expressed by the two different calcite saturations as $\Delta pH_{PHR,CO2\text{-}feed}$ and $\Delta pH_{PHR,CO2\text{-}const}$ values as main results.**

tion pathway shown in Equation 2. All results are based on the consideration of chemical equilibria as calculated in PHREEQC. Changes in CO_2 concentration depending on the fresh water recovery thus have an influence on the H^+ concentration and therefore the pH value. In this way, a validation and possible adjustment of the assumption on CO_2 concentration can be carried out on the basis of pH measurement in real RO processes.

$$CO_{2(aq)} + H_2O \Leftrightarrow H_2CO_3 \Leftrightarrow H^+ + HCO_3^- \Leftrightarrow 2H^+ + CO_3^{-2} \quad \text{(Eq. 2)}$$

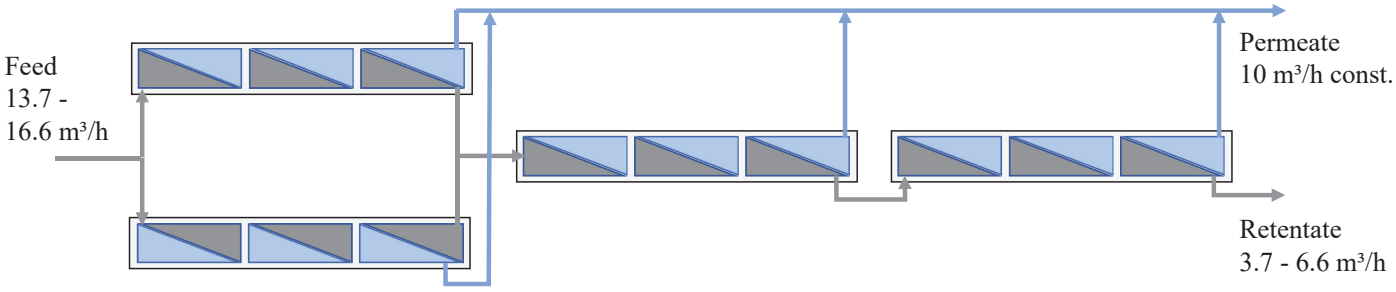

Fig. 3 Reanalysed full scale reverse osmosis system with twelve 8'' low-pressure membrane modules for the investigation of $CaCO_3$ scaling without inhibition. The feed water recovery was varied in the range of 60 to 73 % [13]

Other than for the carbon, the remaining ion composition in the retentate is based on the assumption of 100 % salt rejection as shown in figure 2. Due to the almost 100 % salt rejection of common membranes, this inaccuracy is negligible [21] and will also be neglected in the following for reasons of comparability with the ASTM method. For further application of our simulation approach beyond this work, element- or salt-specific rejection rates can be integrated according to the shown pattern of CO_2 removal in submodel 1 as shown in figure 2.

2.3 Reanalysed full-scale RO data on $CaCO_3$ scaling: Set-up and experimental procedure

Following the calculations with the DIN data set, the calculation of the LSI according to ASTM and our simulation model are transferred to data obtained with a full-scale reverse osmosis plant, as shown in figure 3 [13]. In this study, an antiscalant-free operation of RO plants was investigated at high calcite supersaturation. Up to an LSI of 1.7 the plant could be operated without any antiscalant efforts until $CaCO_3$ scaling could be indicated. In the following we use the extensive raw data of [13] for a reanalysis of the performance data in terms of an early scaling indication. Subsequently, the validity of the obtained LSI values and our calculation method for predicting $CaCO_3$ scaling are evaluated. The RO plant was equipped with twelve 8'' low-pressure reverse osmosis membrane modules in four pressure vessels, as shown in figure 3. The first two pressure vessels were run parallel to maintain recommended flow rates, resulting in three permeate stages. For a comprehensive evaluation of the membrane performance and thus the $CaCO_3$ scaling condition, conductivity, pressure and flow rate were measured before and after every stage. In addition to a temperature measurement, the pH value was also recorded redundantly in the retentate. By gradually increasing the raw water yield from 60 and 73 %, the onset of $CaCO_3$ precipitation was investigated. TMH20A-400 membrane modules from TORAY Industries were used with a nominal membrane area of 37.30 m² per element resulting in about 450 m² membrane surface area. Contrary to common practice [22] or recommendations from the design software TORAY DS2 no acid or other antiscalant was dosed to prevent $CaCO_3$ precipitation and membrane scaling. As is common in the industry, the operation of the plant was controlled to a constant permeate flow. Compliant with the membrane manufacturer's specifications, a permeate flow of 10 m³/h was achieved. The resulting feed flow was between 13.7 and 16.6 m³/h with a retentate flow of 6.6 to 3.7 m³/h depending on the raw water recovery rate. The concentration polarisation factor at the retentate outlet β could thus be kept low and ranged from 1.10 to 1.17 with LSI values from 1.28 to 1.70, all calculated using the manufacturer's design software TORAY DS2 version 2.0.1.58. The composition of the raw water used is shown in table 2. The feed water was at a constant conductivity level between 660 and 670 µS/cm with daily fluctuations in the range of 3 % around the mean value. An ultrafiltration unit was installed prior to the RO system to avoid input of particulate and fouling forming substances. Since the DIN methods do not provide a calculation procedure for the concentration of water by reverse osmosis, only the international standard ASTM and our simulation model are applied to this database.

Table 2 Feed water composition for reanalysing full-scale reverse osmosis data

Paramter	Unit	Value
Calcium	mmol/L	2.99
Magnesium	mmol/L	0.78
Sodium	mmol/L	0.24
Potassium	mmol/L	0.04
Hydrogen carbonate	mmol/L	6.10
Chloride	mmol/L	0.71
Nitrate	mmol/L	0.48
Sulfate	mmol/L	0.28
Temperature	°C	12.2
pH	–	7.31

3 Results

The results are divided into two sections. Firstly, the evaluation of different calculation methods based on the waters of the DIN dataset. This is followed by the transfer of the simulative evaluation of the real data obtained with the full-scale RO plant.

3.1 Calculation results based on the DIN validation dataset

In the following, the simulation results based on the DIN data set are presented. For this purpose, results of the different calculation methods are compared as shown in figure 1. First, we consider the calculated $CaCO_3$ saturation according to the different calculation methods for untreated raw water. On this basis, the predicted water chemistry of simulated RO retentates is then examined.

Table 3 **Water Samples from the German Industry Standard Methods (DIN). The given saturation pH values pH_s were derived from the DIN data set, calculations after ASTM and the PHREEQC model. Based on these values the calcite saturation was expressed as ΔpH**

Paramter	water samples									
	1	2	3	4	5	6	7	8	9	10
pH value of raw water	7.34	7.80	7.00	5.60	7.37	7.86	7.59	7.47	7.30	7.30
saturation Index PHREEQC: SI_{PHR}	−0.39	−0.27	−0.10	−4.15	−0.37	−0.22	−0.54	−0.49	0.11	0.01
saturation pH acc. to DIN: $pH_{S,DIN}$	7.66	8.05	7.08	7.77	7.67	8.06	8.09	7.88	7.23	7.31
saturation pH acc. to ASTM: $pH_{S,ASTM}$	7.98	8.30	7.28	9.98	7.98	8.28	8.32	8.21	7.36	7.25
saturation pH acc. to PHREEQC: $pH_{S,PHR}$	7.65	8.04	7.07	7.76	7.66	8.05	8.08	7.87	7.22	7.29
calcite saturation as ΔpH_{DIN}	−0.32	−0.25	−0.08	−2.17	−0.30	−0.20	−0.50	−0.41	0.07	−0.01
calcite saturation as ΔpH_{ASTM}	−0.64	−0.50	−0.28	−4.38	−0.61	−0.42	−0.73	−0.74	−0.06	0.05
calcite saturation as ΔpH_{PHR}	−0.31	−0.25	−0.07	−2.17	−0.29	−0.19	−0.49	−0.41	0.08	0.01

3.1.1 Calcite saturations based on DIN water samples – comparison of calculation methods DIN, ASTM and PHREEQC

Table 3 shows the main input and results for the determination of calcite saturations based on the ASTM, DIN and our simulation approach with PHREEQC on the DIN water samples. The absence of membrane-based removal of water and degassing shortens our model from figure 2 by the corresponding steps. Corresponding steps were also omitted when using the ASTM method. The various calculated saturation pH values in the calcite equilibrium pH_s can therefore be subtracted with the pH value of the raw water analysis, as shown in table 1, to represent the calcite saturation in pH units as ΔpH (or LSI). This calculated pH difference would have to be overcome to establish equilibrium of the aqueous phase and the solid phase of calcite. Positive ΔpH values mean an oversaturation with calcite. Precipitation is therefore to be expected. However, since kinetic inhibition must be taken into account, this value could be widely exceeded without precipitation. This effect could be described with equilibria of different crystalline forms of $CaCO_3$. For this purpose, the monohydrate MCC and the amorphous form ACC should be further considered besides calcite [23]. Since DIN and ASTM only work with calcite saturation, the following comparisons will only discuss the determined saturations to this crystal form. Table 3 shows the calcite saturations as ΔpH using to the different calculation methods as shown in figure 1. The widely mentioned saturation index SI is only given to complete common data for saturation analysis. As shown in table 3 all given waters in the DIN dataset do not tend to precipitate calcite with the exception of water sample 9. Sample number 9 is supersaturated according to PHREEQC and DIN with 0.07 and 0.08 pH units, whereas ASTM shows an undersaturation with 0.06 pH units. Water sample 10 is almost in perfect equilibrium according to DIN and our calculations in PHREEQC.

The calcite saturation (ΔpH values) of the different calculation methods listed in table 3 are shown in figure 4 as deviations with respect to the ΔpHDIN used as the validation baseline. It is noticeable that our calculation results with PHREEQC are almost identical to those of the DIN validation data set. There is a maximum deviation of 0.02 pH units between the predicted calcite saturations applying these two methods. However, the ASTM method mostly underestimates the calcite saturation by 0.13 to 0.32 pH units. Water sample 4 is an exception in the data set, as it is a relatively soft and acidic water. According to the ASTM, the calcite saturation is even estimated to be 2.2 pH units lower than according to DIN and PHREEQC. Water sample 10 is again an exception with a high temperature of 61 °C. According to ASTM, a slightly higher calcite saturation is to be expected here.

3.1.2 Calcite saturations for simulated RO retentates (ASTM and our sub-models in PHREEQC)

In table 4 we present the results for the prediction of the reverse osmosis retentates applied on the 10 DIN water samples. The feed water recovery and therefore pure water extraction was set to a practical yet sometimes challenging [24] 85 % recovery rate. The calculated calcite saturations according to the ASTM method are compared to our two sub-models for CO_2 degassing through the membrane. Table 4 shows the absolute calcite saturations as ΔpH, the predicted pH values of the retentate and the associated, calculated pH values in calcite equilibrium pHS. With the exception of the soft and acid water no. 4, all waters are distinctly supersatu-

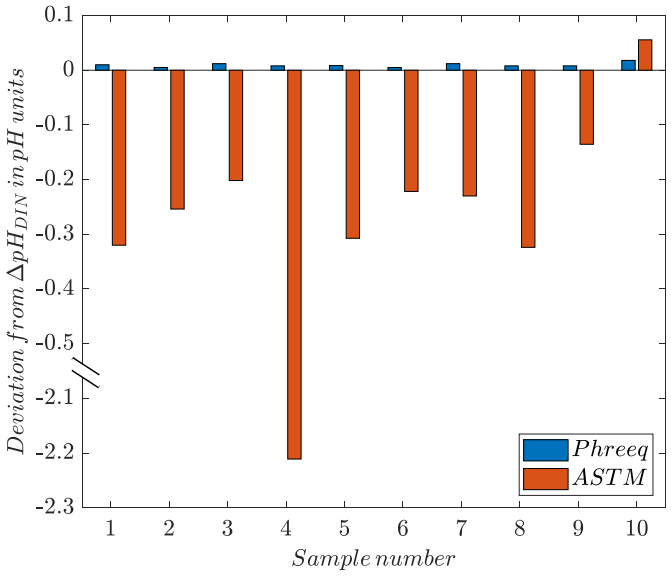

Fig. 4 **Comparison of the calculation results for calcite saturation expressed as ΔpH from DIN in comparison to ASTM and PHREEQC. The values after the DIN method form the baseline. Deviations of the calculation method according to ASTM and PHREEQC are presented in pH units**

Table 4 **Results for the prediction of RO retentates using the 10 DIN waters simulating 85 % feed water recovery. The waters are calculated after the ASTM method and our two sub-models for CO_2 degasification as shown in figure 5**

paramter	water sample									
	1	2	3	4	5	6	7	8	9	10
pH predicted: $pH_{ASTM,CO_2\text{-const}}$	8.12	8.23	7.81	6.30	8.12	8.23	8.22	8.22	8.10	8.10
pH predicted: $pH_{PHR,CO_2\text{-feed}}$	8.00	8.06	7.87	7.75	7.90	7.99	8.02	7.99	7.86	7.59
pH predicted: $pH_{PHR,CO_2\text{-const}}$	8.09	8.54	7.74	6.39	8.12	8.59	8.33	8.22	8.03	8.00
pH at saturation: $pH_{S,ASTM,CO_2\text{-const}}$	6.38	6.72	5.67	8.38	6.38	6.69	6.72	6.61	5.77	5.55
pH at saturation: $pH_{S,PHR,CO_2\text{-feed}}$	6.63	6.82	6.30	7.96	6.64	6.83	6.83	6.77	6.32	6.34
pH at saturation: $pH_{S,PHR,CO_2\text{-const}}$	6.76	7.00	6.40	7.52	6.78	7.04	7.00	6.92	6.44	6.52
calcite saturation as $\Delta pH_{ASTM,CO_2\text{-const}}$	1.74	1.51	2.14	−2.08	1.74	1.54	1.50	1.61	2.33	2.55
calcite saturation as $\Delta pH_{PHR,CO_2\text{-feed}}$	1.37	1.24	1.57	−0.21	1.27	1.16	1.19	1.22	1.55	1.24
calcite saturation as $\Delta pH_{PHR,CO_2\text{-const}}$	1.33	1.54	1.33	−1.13	1.34	1.55	1.33	1.31	1.59	1.49

rated after the extraction of 85 % water. According to the ASTM, the 9 remaining retentates would have to be acidified between 1.50 and 2.55 pH units to achieve at least calcite equilibrium and to prevent scaling in the RO system. A comparison of the different calculation methods for predicting calcite saturation is shown in figure 5. As baseline the ASTM results are used for presentation of the deviation to our two sub-models. According to the ASTM, the saturation is usually much higher than according to our simulations. The soft water no. 4 is estimated to be 1.0 to 1.8 pH units less undersaturated according to our sub-models. The remaining largest differences from the ASTM method are for water samples 1, 3, 5, 9 and 10. In these cases, the ASTM overestimates the calcite saturation by 0.4 to 1.3 pH units. As can be seen in table 4 these large deviations of predicted calcite saturations are mainly due to highly deviating saturation pH values pHS with differences of 0.1 to 1.0 pH units between the ASTM method and our simulation results with PHREEQC. As already shown above in figure 4, this is an indication of an inadequate chemical description of the saturation in the ASTM probably due to the simplifications of the physicochemical principles. Compared to the raw water calculations in figure 4, figure 5 shows predominantly larger discrepancies between the ASTM and our model calculated in PHREEQC. This is probably due to the enhanced salt concentration by the factor 6.66 at 85% recovery rate. Moreover, the deviations of the predicted calcite saturation between our two sub-models indicates the importance of an accurate description of the CO_2 extraction and therefore predicted pH values as listed in table 4. Especially for the relatively soft waters 2, 4 and 6 the predicted pH values differ greatly by 0.5 to 1.4 units between our two sub-models. Therefore, an appropriate model on CO_2 extraction and thus pH prediction is crucial for the design of an operationally safe, i.e. precipitation-free RO process. Both ASTM and our sub-model 2 are based on the assumption of a constant CO_2 concentration from raw water to retentate. Table 4 shows this analogy with a better agreement of ASTM and our sub-model 2 concerning the predicted pH values with constant CO_2 concentration. Only after a reverse osmosis plant had been brought into operation it is possible to supplement the theoretical pH value consideration with measured values. In this paper, the comparison of the pH prediction with the real pH data is discussed below. Most important form figure 5 is the fact, that the ASTM prediction mostly shows high overestimation of the calcite saturation as ΔpH in the range of 0.4 to 1.0 pH units compared to our simulations. In combination with the validation from figure 4 the limited calculation background applied in the ASTM should be critically questioned.

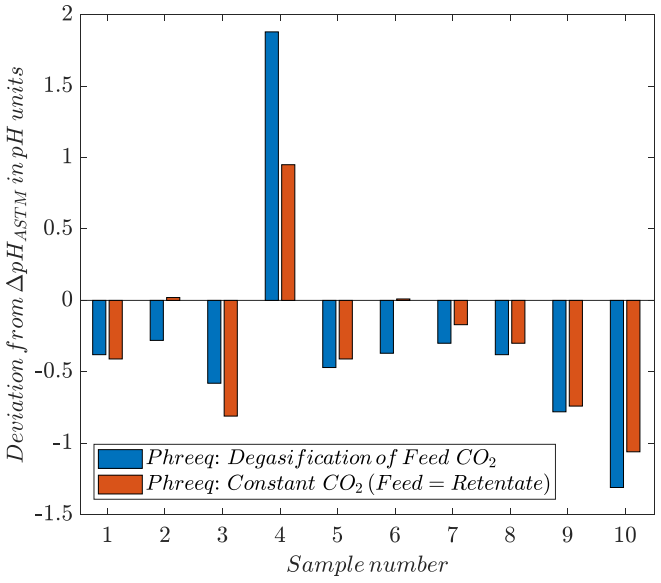

Fig. 5 **Results for the prediction of RO retentates using the 10 DIN waters simulating 85 % feed water recovery. Shown here are the deviations of the calculated calcite saturations according to our two sub-models and the international standard ASTM. The calcite saturation ΔpH_{ASTM} forms the baseline. The absolute calcite saturations are shown in table 4**

3.2 Reanalysis of data from a full-scale RO scaling experiment and simulative prediction

In the following, we combine the prediction of water chemistry of RO retentates with data obtained at the full-scale RO plant. An important validation of the applicability of our hydro chemical simulation is done by testing the pH prediction.

3.2.1 Reanalysis of plant performance data

Figure 6 gives an overview of the experiment with pH values and typical performance indicators. As described above, the pH

measurement at the RO plant was carried out redundantly and permanently in the retentate outlet. The evaluation period was set over 56 days during the stepwise increase of the raw water yield up to a major loss of plant performance. The analysed performance indicators are fresh water recovery, salt passage and water permeability. After 25 days at 60 % recovery, the yield was stepwise increased to 65, 70, 73 and finally 72 % until the termination of the experiment due to a severe performance loss. This is represented by a decreasing membrane permeability of stage 3 from day 50 onwards. The pH values follow each recovery increase stepwise towards higher values, which is an important observation for the choice of a proper CO_2 extraction model. Salt passage and permeability show fluctuations that can be attributed to short interruptions in the operation of the RO plant. Moreover, daily fluctuations become visible. After day 50 salt passage and permeability also decrease that indicates membrane blockage and scaling. The measured pH value serves as a central parameter in the hydro chemical description and is subsequently used to validate our water predictive calculations. A closer look at the quality of the measured pH value is therefore necessary. Both pH measurements in figure 6 show a drift towards elevated values from the initial calibration at day 0. The absolute pH values are therefore associated with an uncertainty. Since the pH values of 60 and 70 % recovery are used in the following for the validation of our prediction approach, an estimation of the values at the recovery increase at day 39 is particular important. The pH electrode 1 shows a mean drift slope of 0.015 pH units per 10 days until day 39. Thus, a total of 0.06 pH units by day 39 could be due to electrode drift caused by interfering factors. Generally, pH measurements are subject to numerous disturbance variables even in the laboratory environment [25]. In general, the pH1 measurement shows more stable values than pH2 and is used in the following discussion with the knowledge of the mentioned uncertainty. Independent of any electrode drift, it is therefore particularly important to consider the trend of stepwise increasing pH values with increasing recovery. By combining the two recovery steps from 60 to 70 %, the pH value jumps in total by 0.10 pH units measured at both electrodes. Also, when recovery is increased to 73 %, another pH step of 0.05 is visible at both electrodes.

A closer examination of the last days of operation of the reverse osmosis system can be seen in figure 7 (see page 62). It is obvious that the salt passage through the membrane decreases from day 50 on until increasing values occur at day 52. The observation of the salt passage serves as a common scaling indicator and increasing values are to be expected by a local increase of the salt concentration at the membrane. Here however, in relation to the range of variation of the salt passage, this course is relatively difficult to interpret. The pH measurements in figure 7 show a continuous decrease from day 49 onwards. From day 50, there is an almost linear decrease to the end with a slope of −0.5 and −0.4 pH units per 10 days for pH1 and pH2. The permeability of the membranes in stage 3 shows a decrease from day 51. Compared to the constant permeability in stage 2, a deterioration of the membrane performance in stage 3 is therefore clear. In addition to the data in figure 6, the meaningful pressure drop in the feed channel via stage 3 could only be extracted from the raw data from day 50 onwards. From day 51 an increasing pressure drop can be observed. Accordingly, the flow resistance in the feed channel in stage 3 increases until the end of the experiment. The deteriorations of the performance data in figure 6 (salt passage, permeability and pressure drop) indicate increasing scaling in stage 3. The decreasing pH values also indicate a deposition, more precisely a deposition of $CaCO_3$. By an approximation of the measured pH values to the lower saturation pHS value, which prevails in calcite equilibrium, this behaviour can be explained. At the given recovery of 73−72 %, the $pH_{S,PHR,CO_2\text{-const}}$ is about 6.5. The sharp decrease from day 49 with pH = 7.8-7.9 is explained by an increasing approach

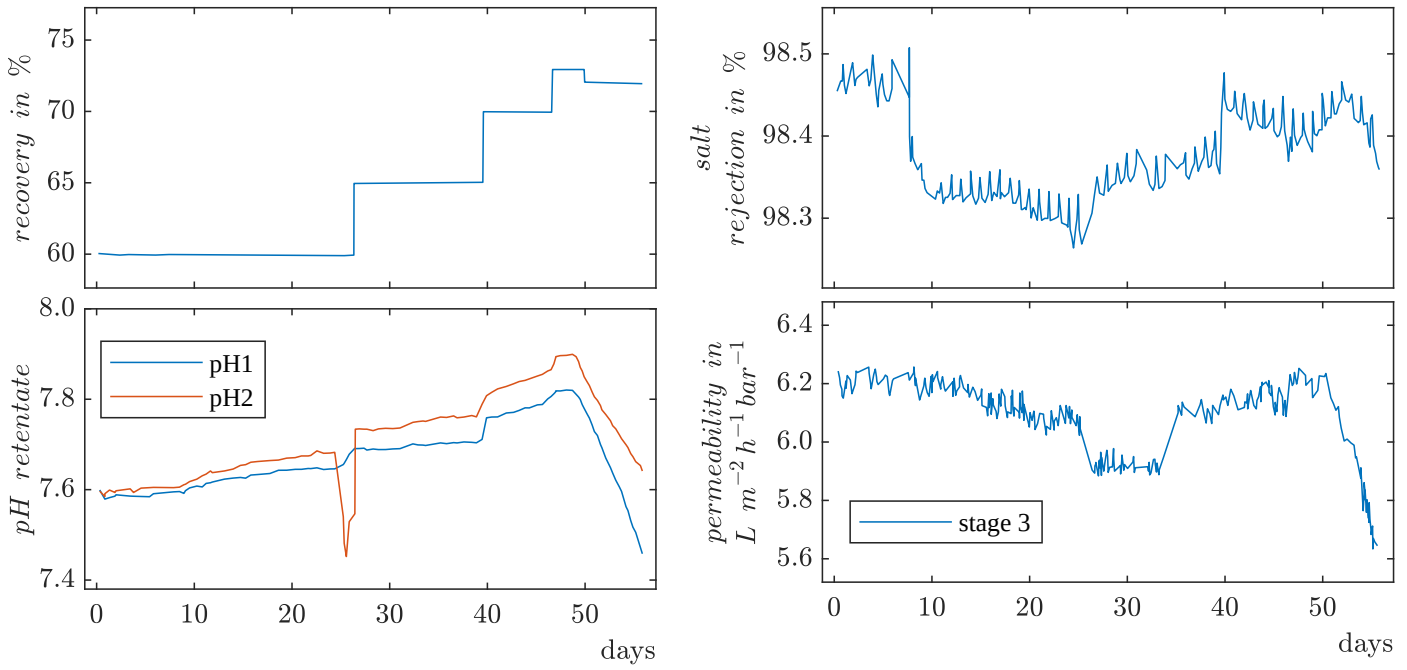

Fig. 6 **Reanalysed performance data of the full-scale reverse osmosis plant for the scaling experiment over 56 days. The data was obtained with a stepwise increase in raw water recovery rate at constant permeate flow without antiscalant efforts**

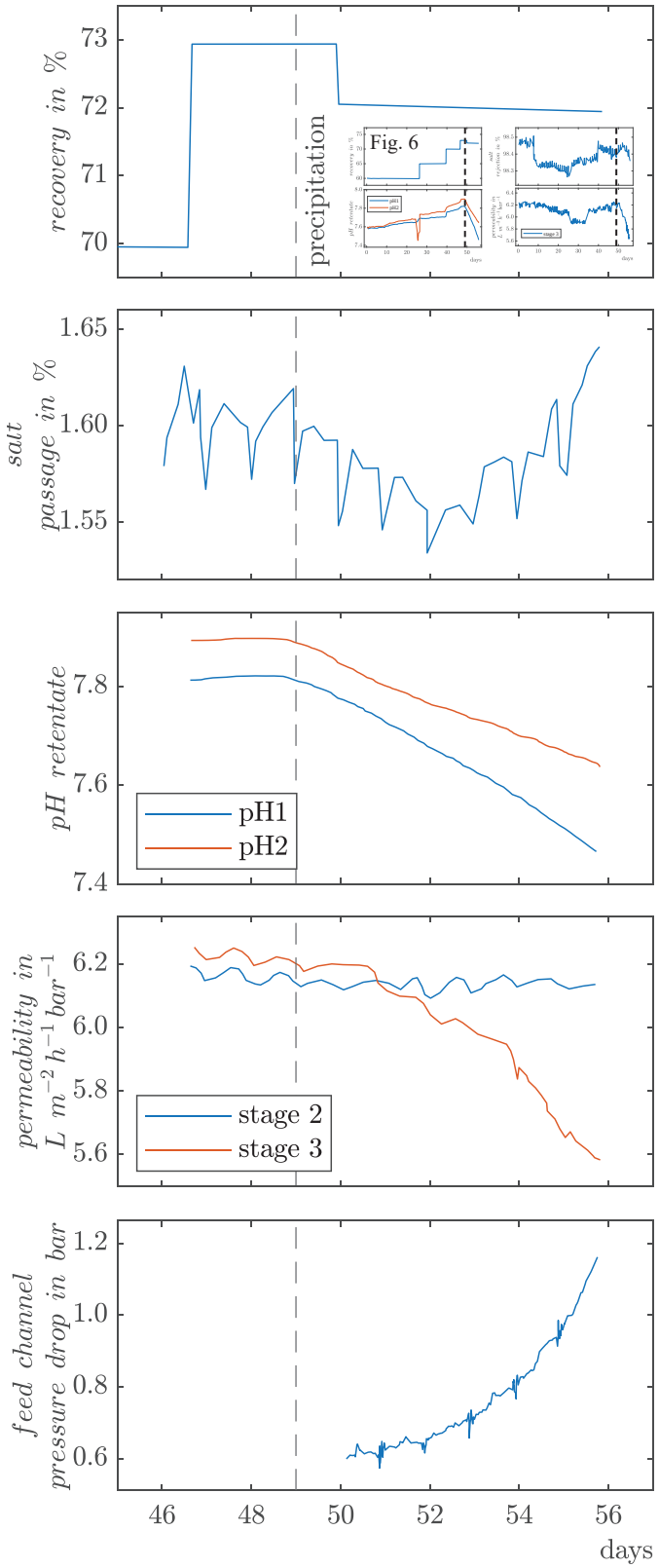

Fig. 7 **Detailed view on the reanalysed performance data of the last days of the scaling experiment with the full-scale reverse osmosis plant**

of the water to the solid $CaCO_3$-phase meaning calcite equilibrium. Due to an increasing $CaCO_3$ precipitation it can be explained that the measured pH values tend more and more towards the lower saturation pHS. This behaviour is also clearly visible in the ever increasing pressure drop. When comparing the pH value and the depicted membrane performance data, it is noticeable that the performance of the membrane only deteriorates from day 51 onwards. However, the water chemistry already changes from day 49, which is visible by the pH drop. From the literature it is known that the mentioned performance data can show membrane scaling only with a certain delay [15]. The pH development is shown here as an early indicator for $CaCO_3$ precipitation. However, the exact location of the start of crystallization in the membrane system cannot be determined with the pH measurement. In combination with the constant permeability in stage 2 and the drop in stage 3, scaling can thus be narrowed down to the last stage, i.e. the last three membrane modules. The crystallization mechanism is unclear at this point. Thus, homogeneous $CaCO_3$ precipitation in the bulk followed by filtrative effect due to the feed spacer could also lead to performance degradation and changes in water chemistry. However, a heterogeneous crystallization mechanism is more likely to be considered with the cautious increase in recovery rate carried out here. The expectable crystallisation zones [1] are discussed in more detail below and support this assumption. The location of highest concentration and scaling probability is expected in the last module at the retentate outlet. It is known that deposits must be expected, especially in the vicinity of the central pipe of membrane modules. Thus, for heterogeneous crystallization, energetically advantageous surfaces are given with the active membrane layer (polyamide) as well as the polypropylene fibres of the feed spacer. In addition, fine particles could be washed in with the feed water and such surfaces also promote heterogeneous crystallization. Due to the ultrafiltration unit prior to the RO system a substantial occurrence of particles is unlikely. Therefore, most likely is an initiation of the crystallisation right at the membrane surface. The average concentration polarization towards the end of the experiment is calculated to be 1.17 times higher than in the bulk [13], which favours precipitation directly on the membrane but also the adjoining surfaces of the spacer fibres. Subsequent to the experimental run analysed here, the plant was exposed to acidic CIP (cleaning in place) cleaning at pH 2 to rinse out the carbonate deposits. In contrast to the initial experimental run analysed above, stable plant operation without $CaCO_3$ scaling could not be achieved in the subsequent experiments, even down to minimum runnable yield of 60 %. From the literature it is known that typical acidic CIP procedures can be incomplete with $CaCO_3$ deposits remaining in membrane systems. In comparative tests with and without the use of antiscalants, poor $CaCO_3$ scaling removal was observed, especially when no antiscalants were used [26] as in this case. The remaining $CaCO_3$ deposits enables a secondary crystallisation pathway as explained in [1].

3.2.2 Evaluation of the quality of our two CO_2-sub-models for predicting the retentate pH value

For further validation of our simulation model and a better understanding of the full-scale data, the experimental results are combined with the water chemistry calculations in the following. The experimental pH data can be used to validate the various calculation methods for carbon rejection. Figure 8 on the left shows the predicted pH values in the retentate according to our two sub-models and the ASTM method compared to the real data. For example, our sub-model 1, which calculates extraction of feed-

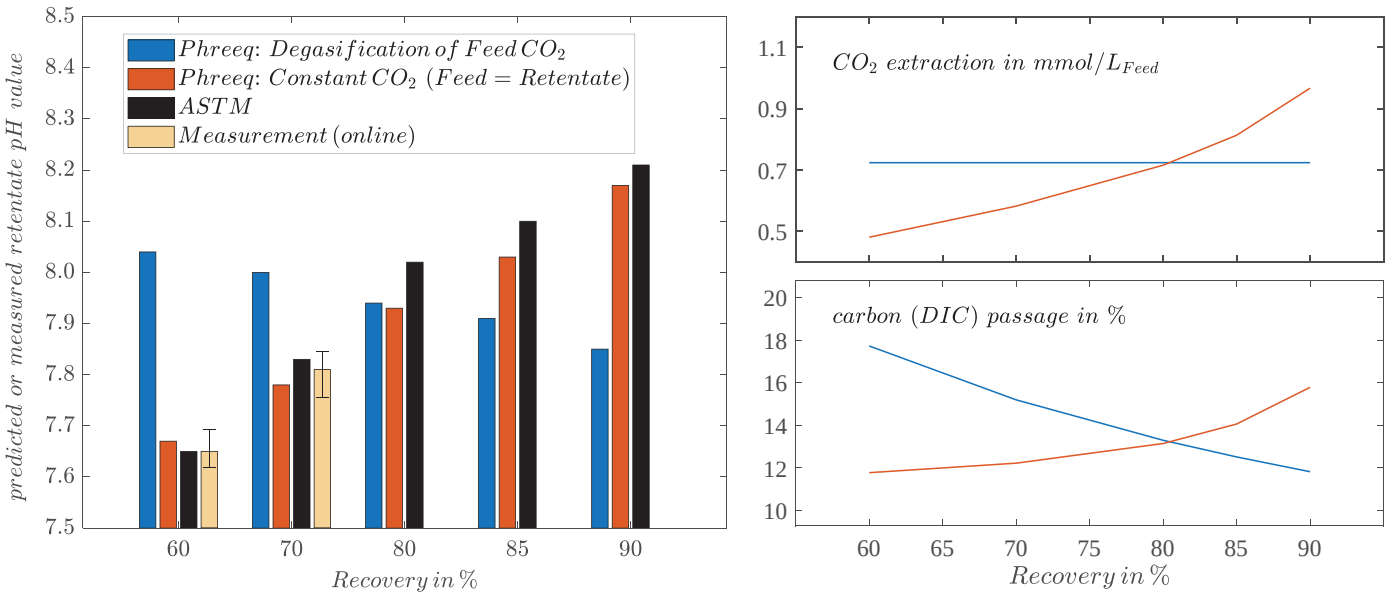

Fig. 8 **Left: Predicted and measured pH values for the retentate of the full-scale reverse osmosis plant at varying feed recovery rates. Above 70 % recovery, no measured values are plotted as scaling and pH drop were indicated at the following recovery step with 73 %. Right: Simulation results for CO_2 extraction based on feed flow and below dissolved inorganic carbon (DIC) passage through the membrane according to our two sub-models**

water CO_2 content independent of recovery rate, shows a predicted $pH_{feed\text{-}CO_2}$ = 8.04 at 60 % recovery, dropping to $p_{Hfeed\text{-}CO_2}$ = 7.85 at 90 % recovery. In contrast, our sub-model 2, which calculates a constant CO_2 content in the retentate independent of recovery rate, shows increasing pH values. Therefore, our sub-model 2 follows the measured pH data of the RO plant analysed in detail above. The ASTM method also shows good pH prediction quality compared to the measured data. Since $CaCO_3$ precipitation was detected at a raw water yield above 70 % with a strong effect on pH, the measured pH data are plotted only up to 70 % in figure 8 on the left. It can be seen that our sub-model 1 including the degassing of the CO_2 content from the feed water deviates relatively widely from the measured values. The pH predictions applying sub-model 2 and ASTM are in good agreement with the measured pH values. It is very noticeable that the gradual increase in pH with increasing recovery rates, are well represented with ASTM and sub-model 2. According to these models, the CO_2 content in the feed and thus in the retentate stream is assumed to be 31.5 mg/L according to PHREEQC and 28.2 mg/L according to ASTM. Based on our sub-model 1, the CO_2 content would be strongly increased with increasing fresh water recovery. At a recovery rate of e.g. 90 % the predicted CO_2 content is calculated to be 68.1 mg/L. This is due to the equilibration of the different carbon species (Equation 2) as the dissolved inorganic carbon (DIC) content increases during the concentrating process. It is therefore useful to consider the resulting CO_2 removal via the membrane and therefore resulting DIC passage through the membrane. This relationship is shown in figure 8 on the right. A constant extraction of the CO_2 content (sub-model 1) results in increasing passage of dissolved inorganic carbon. Salt rejection and therefore salt passage are commonly calculated by a division of permeate and feed concentration [3]. Using the example of the plant operation of the reanalysed data, this relationship can be explained as follows for sub-model 1: According to the plant operation mode “constant permeate flow” an increasing fresh water recovery results from a reduced feed flow. The total amount of CO_2 that can be extracted decreases as a result, and the carbon concentration at constant permeate flow consequently decreases. The DIC passage therefore decreases with increasing yield in sub-model 1. For sub-model 2, an increasing carbon passage can be seen in figure 8 on the right. The CO_2 content can only be kept constant in this model if more and more CO_2 is removed from the feed water with a simultaneous increase in the total carbon concentration due to an increasing fresh water recovery. At about 80 % recovery, the pH and thus the passage of carbon through the membrane is almost similar for both sub-models applied. Besides 80% recovery, the two sub models greatly differ in the amount of extracted carbon, resulting in widely different predicted pH values for the RO retentate. For recovery rates above 80 %, more CO_2 than originally present in the feedwater must be extracted using the sub-model 2. This is only possible if regeneration of CO_2 from the other carbon species present in the retentate solution takes place – mainly HCO_3^- and CO_3^{-2}. The literature confirms the assumption of sub-model 2 that a constant CO_2 content leads to a correct prediction of pH in the retentate [9]. In combination with the high pH prediction quality of sub-model 2, it can be concluded that the assumption of a constant CO_2 content in the feed/retentate stream ensures a good representation of the real situation. Complete CO_2 degassing of the original CO_2 content as in sub-model 1 is not a tenable basis for an accurate simulation of the analysed RO system. According to our sub-model 2 an appropriate prediction above a degassing of the initial/feed CO_2 content is governed a regeneration from other carbon species mainly due to the equilibrium of CO_2, H_2CO_3, HCO_3^- and CO_3^{-2}. In the context of the real data considered here, our modelling approach could be validated with sub-model 2. This chapter shows that the prediction of a constant CO_2 content (sub-model 2) is an appropriate assumption of reality and that there is a substantial DIC passage due to CO_2 extraction through

Table 5 **Predicted and measured values at different feed water recovery rates for the large-scale reverse osmosis system. As the prediction of pH with sub-model 1 fails, the calcite saturations are only listed using a constant CO_2 content according to ASTM and our sub-model 2. The saturation index calculated in PHREEQC is also given to complete data commonly used for saturation analysis**

	recovery rate					
Paramter	**0 %**	**60 %**	**70 %**	**80 %**	**85 %**	**90 %**
pH measured pH_{real}	7.31	7.60–7.68	7.69–7.76	–	–	–
pH predicted ASTM pH_{ASTM}	–	7.65	7.83	8.02	8.10	8.21
pH predicted sub model 1 $pH_{PHR,CO_2\text{-feed}}$	–	8.04	8.00	7.94	7.91	7.85
pH predicted sub model 2 $pH_{PHR,CO_2\text{-const}}$	–	7.67	7.78	7.93	8.03	8.17
saturation pH ASTM $pH_{S,ASTM}$	7.23	6.46	6.21	5.87	5.63	5.28
saturation pH sub model 2 $pH_{PHR,CO_2\text{-const}}$	7.12	6.77	6.66	6.53	6.44	6.32
calcite saturation as ΔpH_{ASTM}	0.08	1.19	1.62	2.15	2.47	2.93
calcite saturation as $\Delta pH_{PHR,CO_2\text{-const}}$	0.19	0.91	1.12	1.40	1.59	1.85
saturation Index $SI_{PHR,CO_2\text{-const}}$	0.27	1.29	1.60	2.01	2.29	2.67

the membrane. In particular, the behaviour at high recovery rates and other plant configurations, e.g. with partial recycling of the retentate stream, should be validated in further studies, since only limited recovery to about 70 % could be validated with the measured data from [13].

3.2.3 Prediction of calcite saturation for the full-scale plant (ASTM and sub-model 2)

In the following the calculated calcite saturations according to the ASTM and our model are discussed. Since the preceding pH-value based validation has shown that the calculations based on constant CO_2 content leads to a high prediction quality, the following will be continued exclusively with the calculation bases from sub-model 2 and the ASTM. Sub-model 1 is excluded because of the poor prediction quality of retentate pH. The raw water used in the reanalysed full-scale experiment is a rather hard tap water, as shown in table 2. It should be noted that this raw water is already supersaturated with calcite regardless of the recovery rate and prediction method. Our model shows good agreement with the membrane manufacturer's software "Toray DS2" with a supersaturation of ΔpH_{PHR} and $\Delta pH_{DS2} = 0.19$. The ASTM indicates a lower supersaturation of the raw water with $\Delta pH_{ASTM} = 0.08$. As described by the ASTM, $CaCO_3$ scaling is to be expected when the ΔpH is exceeded. Therefore, scaling is to be expected already without any concentrating efforts. Figure 9 shows on the left the predicted calcite saturations for the experimental run analysed above over 56 days. According to our sub-model 2, supersaturation is in the range of 0.9 to 1.9 pH units at a fresh water recovery rate from 60 to 90 %. According to the ASTM method, supersaturation is in the range of 1.2 to 2.9 pH units. As above in section 3.1.2 the predicted calcite saturations differ widely between our model and the ASTM method. At 60 % recovery for example, a 0.3 pH unit increased calcite saturation must be expected according to ASTM. The difference between our model and the ASTM increases with increasing recovery. At 90 % yield, for example, the calcite saturation according to the ASTM is already increased by approx. 1.1 pH units compared to our model. To avoid $CaCO_3$ scaling it is

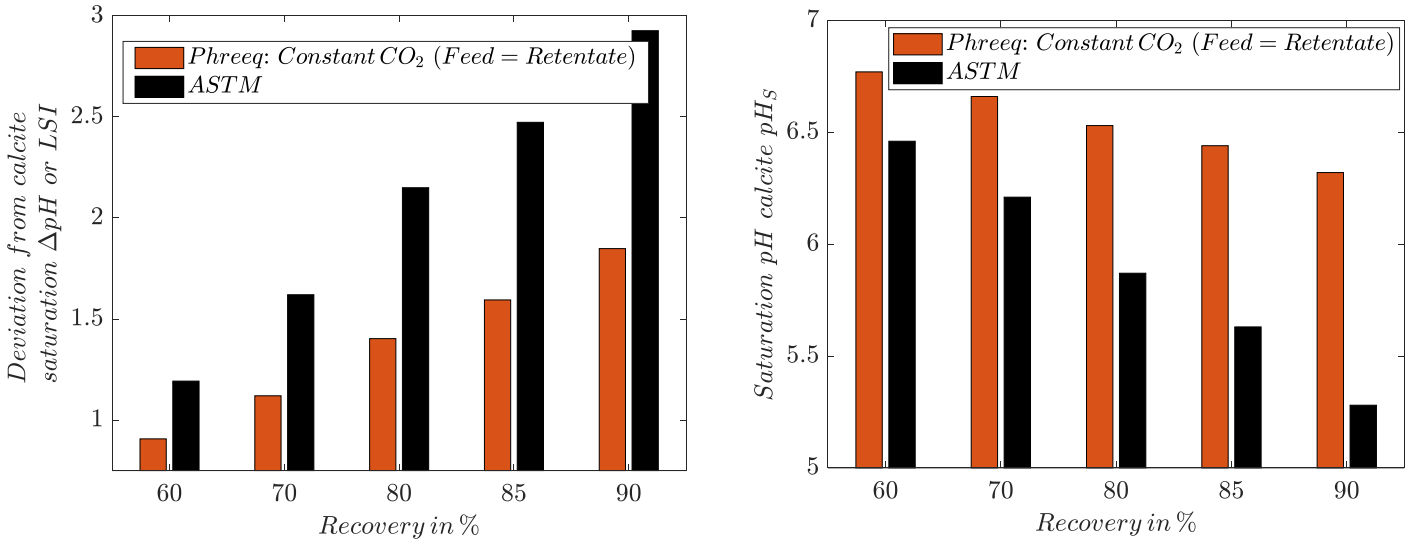

Fig. 9 **Left: Predicted calcite saturation, expressed as ΔpH, for the RO retentate at various feed water recovery rates at the full-scale plant. Due to the above validation, only results for sub-model 2 with constant CO_2 content are shown here. Right: Shows the determined saturation pH values pHS according to the ASTM and our sub-model 2. The differences in the pH_s values show the main reason for the large deviations of the predicted calcite saturations on the left side**

recommended to dose antiscalants or to reduce the supersaturation, for example, by dosing acid [9]. According to the calculation result with the ASTM method, significantly higher concentrations of acid or other scaling inhibitors would have to be added to avoid $CaCO_3$ scaling. The main reason for the widely differing saturation results of ASTM und our model is shown in figure 9 on the right side with the determined saturation pH values pHS. As the calculation of the pH in calcite equilibrium pH_S shows increasing deviations between ASTM and our model with increasing recovery. As shown in the basic Equation 1 for the pH-based description of calcite saturation ΔpH, the predicted pH value subtracted by the saturation pH value pH_S. As discussed above and shown in table 5, there is a maximum deviation of about 0.1 in predicted pH values between our sub-model 2 and the ASTM. The large deviations of the saturation results (ΔpH_{ASTM} and $\Delta pH_{PHR,CO_2\text{-const}}$) are therefore mainly due to the deviation in the calculated pHS values, as shown in figure 9 on the right. As discussed above, calculations with the DIN data also show comparatively large deviations for waters 3 and 9, which have a similar degree of hardness to the water in the full-scale test. As explained before, it is reasonable to assume that our model reflects the real situation better than the ASTM due to the comprehensive physicochemical approach and conformity with the comprehensive DIN method. Therefore, the method presented in the international standard ASTM could greatly overestimate calcite saturation. The results of the design software DS2 of the membrane manufacturer and antiscalant supplier TORAY Industries shows similar differences to our model. For example, the predicted calcite saturation as LSI or ΔpH_{DS2} for 60 and 70 % recovery are close to the ASTM results with 1.3 and 1.7 pH units versus 1.2 and 1.6 according to the ASTM. For example, at 60 and 85% recovery, the ASTM and DS2 software show increased calcite saturation compared to our sub-model 2 of about 0.3/0.4 and 1.0/1.1 pH units, respectively. This overestimation of calcite saturation is in accordance with the literature, as it is known that calcite saturation has been overestimated by various membrane supplier design software [12].

Regardless of which method is used to calculate calcite saturation, a permanent supersaturation in the analysed full-scale experiment can be derived from table 5 and figure 9, left. Increasing supersaturations, that is, positive ΔpH values, are expected to have an increasing tendency to form calcium carbonate precipitation. As analysed above and confirmed in [13], scaling could be indicated from a raw water yield of 73 %. Calcite was thus supersaturated by $\Delta pH_{PHR,CO_2\text{-const}}$ = 1.2 according to our validated sub-model 2. Even at the lowest recovery rate of 60 %, which was operated 3.5 weeks without any signs of scaling, a strong supersaturation of $\Delta pH_{PHR,CO_2\text{-const}}$ = 0.9 was present. Therefore and due to different crystallisation zones of $CaCO_3$ explained in [1], the use of calcite saturation for the prediction of $CaCO_3$ precipitation propensity seems not suitable.

3.2.4 Determination of different crystallisation zones with a saturation prediction of $CaCO_3$ polymorphs

As explained elsewhere [23, 27], the $CaCO_3$ polymorphs calcite, MCC and ACC are crucial for the representation of different crystallization zones of $CaCO_3$ and a metastable region. Figure 10 shows the respective saturations for the full-scale RO experiment

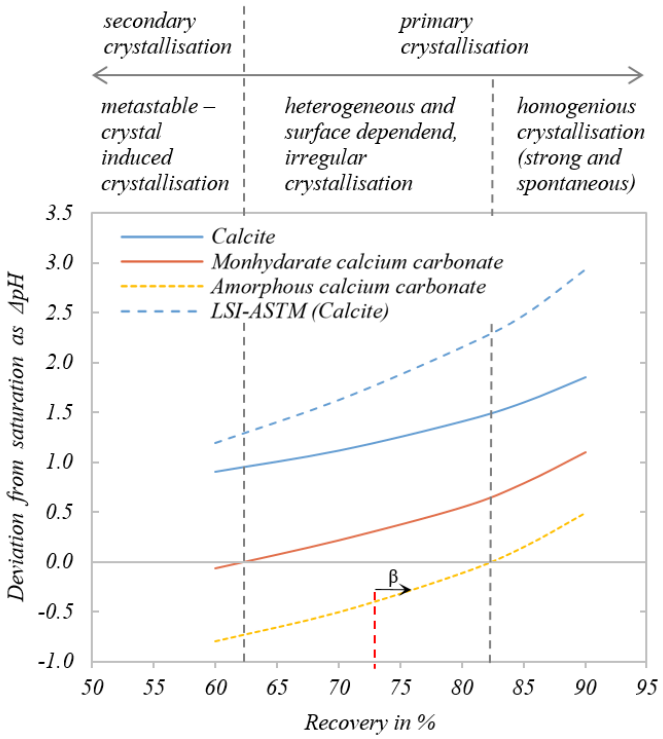

Fig. 10 Simulation results applying our sub-model 2 for the determination of $CaCO_3$ saturations as ΔpH of different polymorphs dependent on the recovery rate. The monohydrate and amorphous $CaCO_3$ (MCC and ACC) are used besides calcite for the identification of crystallization zones and scaling propensity. The reanalysed full-scale experiment was thus mainly carried out in the zone of heterogeneous, irregularly occurring crystallization between 62 and 73 % recovery. At 73 % the detected start of $CaCO_3$ precipitation is marked. Here, the influence of the concentration polarization β on the saturation curve of ACC is illustrated as an example

analysed in this study. All saturations were calculated using the previously validated CO_2/pH prediction with sub-model 2. Figure 10 shows a permanent supersaturation of calcite as $\Delta pH_{PHR,CO_2\text{-const}}$ from 0.9 to 1.2 pH units according to our model and for comparison the ASTM/LSI values for as already discussed in chapter 3.2.3. The more soluble monohydrate MCC is only supersaturated from a feed water recovery of 62 %. Above this recovery rate, the zone of heterogeneous crystallization is reached. A slow and not always starting heterogeneous crystallization can be expected following the laboratory experiments of Elfil et al. [23, 27]. The amorphous $CaCO_3$ ACC gets supersaturated at about 82 % recovery according to our model. Above this level, a strong, spontaneous and reliably occurring crystallization must be expected – independent of energetically advantageous surfaces in the membrane system and fluid flow. The analysed full-scale plant was operated at 60% recovery for about 25 days. The MCC is slightly undersaturated at this yield and calcite is strongly supersaturated. In this saturation range, only crystal-induced $CaCO_3$ crystallization can be expected. Since new membrane modules and generally new plant equipment was installed, residues of crystal precipitation can be excluded in this experimental phase and $CaCO_3$ precipitation could not be expected. In the following 30 days of the experiment, the yield steps of 65, 70, 72 and 73 % were all run in the range of MCC supersaturation and ACC undersaturation. Thus, the RO system was operated in a zone where a slow, irregular and surface-

Table 6 Main results of this study comparing the ASTM, DIN and our simulation model for the prediction of calcite saturations of reverse osmosis retentates

results based on DIN validation data set			results based on full-scale RO data		
calcite saturation of raw waters	**calcite saturation of simulated retentates**	**pH prediction of simulated retentates**	**prediction of pH value**	**calcite saturation**	**integration of $CaCO_3$ polymorphs**
ASTM ≠ DIN = PHR ↑ comprehensive physicochemical basics	ASTM >> PHREEQC (7 of 10 waters)	$PHR_{CO_2\text{-feed}} \neq PHR_{CO_2\text{-const.}} \approx$ ASTM	$PHR_{CO_2\text{-feed}} \neq PHR_{CO_2\text{-const.}} \approx$ ASTM ≈ real data	ASTM >> $PHR_{CO_2\text{-const}}$ ($PHR_{CO_2\text{-cons}}$ excluded due to poor pH prediction)	successful representation of $CaCO_3$ crystallization zones (based on $PHR_{CO_2\text{-const}}$)

- DIN an PHREEQC with high level of physicochemical description of calcite saturation in good agreement
- Full-scale data show high prediction quality with our sub-model 2 ($PHR_{CO_2\text{-const}}$) for pH/CO_2 prediction
- Integration of polymorphism (MCC, ACC saturation) of $CaCO_3$ successful and reasonable in terms of scaling behaviour of analysed full scale scaling experiment

➜ Our sub-model 2 ($PHR_{CO_2\text{-const}}$) with the integration of $CaCO_3$ polymorphism can serve as high quality prediction tool for RO retentate water chemistry and $CaCO_3$ saturation resp. scaling propensity

dependent heterogeneous crystallization has to be expected. Recovery rates at which strong and spontaneous precipitation of $CaCO_3$ would be expected were therefore not run in the analysed experiment. Also when including the concentration polarisation β the ACC saturation was not reached at 73 % recovery. The effect of β is shown in figure 10 as an example for this relationship. At 73 % recovery the concentration factor due to water extraction is about 3.7 which can be multiplied by β = 1.17, resulting in a total concertation factor of 4.3. Calculated back to the recovery rate, this concentration factor is reached at 77 % which leads to an increase of MCC saturation of 0.15 pH units right at the membrane surface. Continuing, ACC saturation was not reached at the maximum recovery rate. Therefore, a locally initiated, spontaneous nucleation cannot be expected. Similarly, at 60% recovery, the effect of β = 1.10 leads to a notional yield increase of about 4 %, resulting in a local increase in MCC saturation of about 0.10 pH units. The crystallization zone at 60 % yield is thus not clearly delineated. Including β, it can be assumed that primary/heterogeneous crystallisation is already possible directly at the membrane at 60 % recovery rate. Independent of the influence of concentration polarisation, it is clear from the high calcite supersaturation that possibly existing $CaCO_3$ crystals present cause precipitation/scaling in this area. In chapter 3.2.1, the connection between CIP and an expected incomplete cleaning of crystal residues has already been explained. Therefore, it is expected that after one-time $CaCO_3$ scaling, the secondary crystallization mechanism prevails in RO systems. The repeated experiments in the range between 60 and 70 % yield all led to immediate precipitation and can be explained by the explained by this energetically advantageous crystallisation mechanism compared to the initial experiment within the primary crystallization zone. The consideration of the crystallization zones is up to this point a strongly idealized consideration and therefore only a one-rationing of the propensity of $CaCO_3$ scaling. In fact, in real applications, numerous and complex influences on scaling development must be expected [15]. The crystallisation zones in figure 10 refer to the laboratory boron environment and pure calcium carbonate systems [23, 27]. For natural waters, precipitation is expected to be subject to various inhibitory effects. The presence of divalent cations as magnesium is known to inhibit calcite precipitation and alter the crystallisation mechanism [28, 29]. In addition, organic acids such as fulvic acids and humic acids cannot be excluded in natural waters, which also have an inhibitory effect on the precipitation of calcium carbonate, even in the micro molar range [28]. Thus, the MCC and ACC saturation shown in figure 10 could be shifted towards higher concentrations by various inhibitory effects. The complex flow field in the narrow feed channel (approx. 0.7–1.2 mm height) with crossing spacer fibres can in turn cause locally elevated concentrations beyond the mean concentration polarisation β. Additionally, in the common operation of reverse osmosis systems, anti-scale agents are dosed, e.g. on the basis of phosphonates [13]. Such substances are intended to prevent e.g. the deposition of $CaCO_3$. However, when increasing the recovery rate of waters containing calcium and dissolved inorganic carbon, a limit is always reached at which $CaCO_3$ precipitations occurs. With the strong, spontaneous, and repeatable detectable crystallization above ACC saturation known form the literature [27], an important upper limit for a successful $CaCO_3$ stabilization could be given. The recommendation from Toray industries, for example, is not to exceed an LSI of 2.2 even when using antiscalants to avoid $CaCO_3$ precipitation. As shown in figure 10, this LSI level is reached at about 80 % recovery. Incipient ACC supersaturation also occurs in this range at about 82 % recovery. Further studies could investigate whether ACC saturation marks a limit at which conventional antiscalants can no longer fulfil their precipitation-preventing function. Most important in this section is the fact that the simple relationship of $\Delta pH_{Calcite} > 0$ is not a sufficient parameter for the determination of scaling propensity, since it is only meaningful in the presence of crystals on which secondary crystallization takes place. Otherwise, the primary pathway and therefore the $CaCO_3$ polymorphism plays a decisive role for the formation of $CaCO_3$ scaling. These interrelationships can be represented with our presented simulation model.

4 Conclusion

With this study, a simulation basis was created and tested, which is suitable for the prediction of the water chemistry of RO retentates. The prediction of the calcite saturation was distinguished from the current standardization and extended to include the influence of the $CaCO_3$ polymorphs MCC and ACC describing different crystallization zones. Table 6 and the following text present the main findings of this study.

The calculated calcite saturations are based on comprehensive chemical principles using the hydro chemical software PHREEQC and are in good agreement with the DIN within the validation data set for raw waters supported. The ASTM standard uses simpler backgrounds for the determination of calcite saturation and deviates from the well-founded calculations according to DIN and PHREEQC. The ASTM method indicates decreased saturations in the range of 0.2 to 0.3 pH units (LSI) for the raw waters of the DIN validation data set. Only for a particular soft and another 61 °C hot water of the DIN data set, this pattern is interrupted. DIN and PHREEQC remain in good agreement, the ASTM method shows results deviating by up to 2.2 pH units.

For predicting the water chemistry of RO retentates, we tested two sub-models. Our sub-model 2, calculating a constant CO_2 content independent of raw water yield, was found to be accurate based on data of a full-scale RO system. The appropriate pH prediction of the retentate, indicating the carbon passage through the membrane, therefore provides a good description of the carbonate chemistry of RO retentates with our sub-model 2. Sub-model 1, which calculates the total removal of the raw water CO_2 content, could not provide a good fit with the real data and is excluded in the following discussion. Sub-model 2 is thus consistent with the literature and recommendations of the ASTM international standard for the prediction of RO retentates.

However, the ASTM results in increased saturation values in comparison to our sub-model 2 with simulative concentrated DIN water samples as well as with the retentate from the full-scale plant. In particular, the relatively hard waters 3 and 9 of the DIN data set and the hard water from the reanalysed full-scale data show large deviations of the calculated calcite saturations in the range of 0.8–0.9 pH units. This means a large difference in acceptable fresh water recovery for a save prevention of $CaCO_3$ scaling. For example, according to our calcite model, the difference of 0.8 pH units would be covered by a jump from 60 to over 85 % recovery. Since the ASTM uses a simplified approach compared to DIN and our model, we have to assume an overestimated representation of the calcite saturation according to ASTM. The large deviation of the ASTM and our model occurs in the determination of the saturation pH value pHS. The predicted retentate pH values show only minor differences between the ASTM method and our model.

A major improvement in the prediction of $CaCO_3$ scaling propensity is given in this work with the incorporation of saturation of $CaCO_3$ polymorphs besides calcite in our simulation model. Our calculations for MCC saturation can be interpreted according to the literature as a potential starting level of crystallization of $CaCO_3$ in clean i.e. crystal-free environment. Our calculations for ACC saturation are then used to describe a hard limit above which spontaneous and strong crystallization can be expected. The conventional consideration of the calcite saturation is only relevant if crystal surfaces for the energetically advantageous secondary crystallization are already present due to preceding crystal input or residues. Our analyses confirm the literature with scaling data from a full-scale RO plant, to the extent that calcite solubility alone, is not an accurate parameter for predicting $CaCO_3$ scaling. The polymorphism of $CaCO_3$ should be given greater attention in this context. Our analyses also confirmed the literature in that an indication of $CaCO_3$ precipitation occurs in a clean and crystal free system after calcium carbonate monohydrate (MCC) saturation is exceeded.

According to our results, a critical recovery in terms of $CaCO_3$ precipitation in RO systems could be significantly higher than indicated on the basis of the international standard ASTM and membrane manufacturer software. The DIN and our simulation model are based on more extensive physicochemical backgrounds than the ASTM method to describe the $CaCO_3$ saturation. For concentrated drinking waters from the DIN validation data set, it could be shown that the saturations for calcite are mostly much lower than described by the usual LSI. Based on the depiction of freshwater yield-dependent crystallization zones, it should be possible to derive ranges of different requirements for antiscalant dosages. Up to MCC saturation, crystal-free RO systems should be able to be operated completely without antiscalant. Above MCC saturation, a dosage is always required to reliably prevent precipitation. Systems in which precipitation has already occurred should be operated with antiscalant already from the saturation of calcite since CIP cleaning is not expected to completely clean off crystal residues. Beyond this work with the explained uncertainties in the purely simulative description of the scaling propensity, the following Part III will deal with scaling detection in more detail. Here, for the first time, the integration and results with a polymer optic fibre sensor in a reverse osmosis system will be presented. Such sensor data extend the monitoring capability of RO systems and offer the possibility of sensitive and early monitoring of the actual onset of scaling and precipitation and could be used to better understand the complex scaling phenomena.

5 References

1. Hager, S.; Bachmann, A.; Hofmann, T.; Engelbrecht, R. and Glas, K.: $CaCO_3$ deposits in reverse osmosis: Part I – Shortcomings of current approaches leading to a new prediction model and monitoring device, BrewingScience, **74** (2021), no. 9/10 pp. 122-133.
2. Ruiz-García, A. and Feo-García, J.: Estimation of maximum water recovery in RO desalination for different feedwater inorganic compositions, Desalination and Water Treatment, **70** (2017), pp. 34-45.
3. Crittenden, J. C.; Trussell, R. R.; Hand, D. W.; Howe, K. J. and Tchobanoglous, G.: MWH's Water Treatment: Principles and Design, 3rd ed., John Wiley and Sons, Hoboken, N.J, 2012.
4. Antony, A.; Low, J. H.; Gray, S.; Childress, A. E.; Le-Clech, P. and Leslie, G.: Scale formation and control in high pressure membrane water treatment systems: A review, Journal of Membrane Science, **383** (2011), no. 1-2, pp. 1-16.
5. Dupont: FilmTec™ Reverse Osmosis Membranes Technical Manual, 2022, https://www.dupont.com/content/dam/dupont/amer/us/en/water-

solutions/public/documents/en/45-D01504-en.pdf.
6. Peña, J.; Buil, B.; Garralón, A.; Gómez, P.; Turrero, M. J.; Escribano, A. et al.: The vaterite saturation index can be used as a proxy of the S&DSI in sea water desalination by reverse osmosis process, Desalination, **254** (2010), no. 1-3, pp. 75-79.
7. Ruiz-Saavedra, E.; Ruiz-García, A. and Ramos-Martín, A.: A design method of the RO system in reverse osmosis brackish water desalination plants (calculations and simulations), Desalination and Water Treatment, **55** (2014), no. 9, pp. 1-11.
8. Thompson, J. F.: Membrane Mineral Scaling and its Mitigation in Reverse Osmosis Desalination of Brackish Water, Dissertation, 2017.
9. ASTM International: Standard Practice for Calculation and Adjustment of the Langelier Saturation Index for Reverse Osmosis D3739 – 19.
10. Langelier, W. F.: The analytical control of anti-corrosion water treatment, Journal - American Water Works Association, **28** (1936), no. 10, pp. 1500-1521.
11. Ruiz-García, A. and La Nuez-Pestana, I. d.: A computational tool for designing BWRO systems with spiral wound modules, Desalination, **426** (2018), pp. 69-77.
12. Waly, T.; Kennedy, M. D.; Witkamp, G.-J.; Amy, G. and Schippers, J. C.: Predicting and measurement of pH of seawater reverse osmosis concentrates, Desalination, **280** (2011), no. 1-3, pp. 27-32.
13. Müller, U.; Groß, H.; Willbold, H.; Meinardus, M. and Friedrichowitz, G.: Potentiale der elektrochemischen Scaleinhibierung bei Membrananlagen in der zentralen Trinkwasseraufbereitung und deren Umsetzung an einer Demonstrationsanlage: Abschlussbericht DVGW-Förderkennzeichen W 4-02-12, 2015.
14. Parkhurst, D. L. and Appelo, C. A. J.: Description of Input and Examples for PHREEQC Version 3: A Computer Program for Speciation, Batch-Reaction, One-Dimensional Transport, and Inverse Geochemical Calculations, book 6, chapter A43, 2013, https://pubs.usgs.gov/tm/06/a43/, accessed March 6, 2017.
15. Karabelas, A. J.; Mitrouli, S. T. and Kostoglou, M.: Scaling in reverse osmosis desalination plants: A perspective focusing on development of comprehensive simulation tools, Desalination, **474** (2020), p. 114193.
16. Deutsches Institut für Normung e. V.: German standard methods for the examination of water, waste water and sludge - Physical and physico-chemical parameters (group C) – Part 10: Calculation of the calcit saturation of water (C 10), 13.060.60, 38404-10:2012-12, Beuth Verlag, Berlin, 2012.
17. Amjad, Z. and Demadis, K. D. (Eds.): Mineral scales and deposits: Scientific and technological approaches, Elsevier, Amsterdam, 2015.
18. Pitzer, K. S.: A thermodynamic model for aqueous solutions of liquid-like density, Reviews in Mineralogy, 1987.
19. Lu, P.; Zhang, G.; Apps, J. and Zhu, C.: Comparison of thermodynamic data files for PHREEQC, Earth-Science Reviews, **225** (2022), p. 103888.
20. Moel, P. J. de; van der Helm, A. W. C.; van Rijn, M.; van Dijk, J. C. and van der Meer, W. G. J.: Assessment of calculation methods for calcium carbonate saturation in drinking water for DIN 38404-10 compliance, Drinking Water Engineering and Science, **6** (2013), no. 2, pp. 115-124.
21. Proc. 25th International Conference on Plastic Optical Fibers.
22. Shahid, M. K. and Choi, Y.: Sustainable Membrane-Based Wastewater Reclamation Employing CO_2 to Impede an Ionic Precipitation and Consequent Scale Progression onto the Membrane Surfaces, Membranes, **11** (2021), no. 9.
23. Elfil, H. and Roques, H.: Role of hydrate phases of calcium carbonate on the scaling phenomenon, Desalination, **137** (2001), no. 1-3, pp. 177-186.
24. Gilron, J.: Brine Treatment and High Recovery Desalination, Emerging Membrane Technology for Sustainable Water Treatment, Elsevier, 2016, pp. 297-324.
25. Deutsches Institut für Normung e. V.: pH-measurement – pH-measurement of aqueous solutions with pH measuring chains with pH glass electrodes and evaluation of measurement uncertainty, 71.040.40, no. 19268, Beuth Verlag, Berlin, 2021.
26. Shahid, M. K.; Pyo, M. and Choi, Y.-G.: The operation of reverse osmosis system with CO_2 as a scale inhibitor: A study on operational behavior and membrane morphology, Desalination, **426** (2018), pp. 11-20.
27. Elfil, H. and Roques, H.: Prediction of the limit of the metastable zone in the "$CaCO_3$-CO_2-H2O" system, AIChE Journal, **50** (2004), no. 8, pp. 1908-1916.
28. Appelo, C. A. J. and Postma, D.: Geochemistry, groundwater and pollution, 2nd ed., CRC Press, Boca Raton, 2013.
29. Loste, E.; Wilson, R. M.; Seshadri, R. and Meldrum, F. C.: The role of magnesium in stabilising amorphous calcium carbonate and controlling calcite morphologies, Journal of Crystal Growth, **254** (2003), no. 1-2, pp. 206-218.

Received 30 June 2022, accepted 22 July 2022